

Stability of Borane–Adduct Complexes: A G-2 Molecular Orbital Study

Hafid Anane and Abderrahim Boutalib*

Département de Chimie, Faculté des Sciences Semlalia, Université Cadi Ayyad, B.P. S15 Marrakech, Morocco

Francisco Tomás

Departament de Química Física, Universitat de València, Dr. Moliner 50 E-46100, Burjassot, València, Spain

Received: April 17, 1997; In Final Form: July 14, 1997[⊗]

Complexation energies of H_3BXH_n and $[H_3BXH_{n-1}]^-$ complexes ($X = N, O, F, P, S,$ and Cl) ($n = 3, 2, 1$) have been computed at the G-2 level of theory. The formation of H_3BXH_3 ($X = N, P$) is found to be more favored than the formations of H_3BXH_2 ($X = O, S$) and H_3BXH ($X = F, Cl$). The qualitative features of the molecular orbital interaction (the correlation diagrams) of H_3BNH_3 (C_{3v} symmetry group), H_3BOH_2 (C_s symmetry group), and H_3BFH (C_s symmetry group) complexes are presented. These diagrams show that the σ character of the B–X bond decreases and the π character increases when the electronegativity of X increases and indicate that the B–X bond cannot be treated only in terms of the simplest model of the HOMO–LUMO interaction (i.e., a two-level and two-electron model system). Two linear correlations were established and discussed. The first one was between proton affinities of the Lewis bases L ($L = XH_n$ and $[XH_{n-1}]^-$, $n = 3, 2, 1$) and complexation energies of the H_3BL compounds calculated at the G-2 level of theory. The second correlation was between the ^{11}B NMR coupling constant $^1J_{B-H}$ and the complexation energies of H_3BL ($L = OH^-, PH_2^-, SH^-, Cl^-, NH_3,$ and PH_3).

1. Introduction

Donor–acceptor complexes between Lewis acids and bases play a very important role in many catalytic reactions.^{1,2} The knowledge of the structure and properties of these complexes is a necessary goal for understanding the mechanism of such processes.

Diborane (B_2H_6) chemistry has long been a very active field of research as a consequence of its unusual structure and bonding.^{3–5} It reacts readily with a range of Lewis bases, in both solution and gas phase. Recently, a series of papers appeared on the pyrolysis of the diborane with $NH_3, PH_3, SH_2, CH_3NH_2, CH_3OH,$ and $CH_3SH,$ leading to selective formation of aminoborane,⁶ phosphinoborane,⁷ mercaptoborane,⁸ methylaminoborane,⁹ methoxyborane,¹⁰ and methylmercaptoborane,¹¹ respectively. It was concluded from these results that aminoborane, phosphinoborane, and mercaptoborane were produced through borane–Lewis base adducts. The authors proposed a two-step mechanism. The first step is the slow formation of a borane–Lewis base adduct (H_3BL), and the second is the rapid hydrogen elimination from the H_3BL compound. On the other hand, the possible pathways for these reactions have been thoroughly investigated using ab initio methods.¹² The conclusion is that the energy barrier height for the hydrogen elimination from the adduct H_3BXH_n is proportional to the values of proton affinity of the Lewis bases XH_n ($X = N, O, S,$ and $P; n = 1–3$). It is also concluded that the adduct complexation energies are related completely to the nature of Lewis bases. Furthermore, Morokuma and co-workers¹³ have explained the stabilities of electron donor–acceptor complexes $H_3BCO, H_3BNH_3, H_3BNH_2(CH_3), H_3BN(CH_3)_3,$ and H_3NBF_3 in terms of electrostatic, exchange, polarization, and charge-transfer contributions to the interaction energy. Glendening and Streitwieser,¹⁴ using the natural energy decomposition analysis (NEDA), which is based on the natural bond orbital (NBO) procedure, reported

that H_3BCO and H_3BNH_3 complexes are significantly stabilized by charge-transfer interaction. In the case of Lewis acid–base complexes of $BH_3, BF_3, BCl_3, AlCl_3,$ and $SO_2,$ Frenking et al.¹⁵ showed that the bonding in the strongly bound donor–acceptor complexes ($H_3BCO, H_3BNH_3, H_3BNMe_3, F_3BNH_3, F_3BNMe_3, Cl_3BNH_3,$ and Cl_3BNMe_3) have large covalent contributions while the bonds in the more weakly bound complexes ($F_3BCO, F_3BNCH, Cl_3BCO, Cl_3BNCMe, Cl_3AlOClEt, Cl_3AlNMe_3,$ and Me_3NSO_2) are dominated by electrostatic interactions. They also showed that electrostatic interactions are dominant in the strongly bound complex $Cl_3AlNMe_3,$ while the related complex H_3BNMe_3 is mainly bound by charge-transfer interactions. For H_3BCO and $H_3BNH_3,$ they concluded also that the donor–acceptor bond of these complexes has a higher covalent character. Moreover, the H_3BNH_3 complex is more strongly bound than the H_3BCO complex because the Coulomb interactions are stronger in H_3BNH_3 than in $H_3BCO.$ Another study by Dapprich and Frenking,¹⁶ using the charge decomposition analysis (CDA), reported strong electron donation from CO to BH_3 (0.550 e at MP2/6-31G(d)) and significant back-donation from BH_3 to CO (0.253 e at MP2/6-31G(d)) for the H_3BCO complex and strong electron donation from NH_3 to BH_3 (0.382 e at MP2/6-31G(d)) but no back-donation from BH_3 to $NH_3.$ Recently, Skancke et al.¹⁷ concluded that the successive fluorine substitutions on boron or nitrogen reduce the complex binding energies and showed that the charge transfers are correlated with the degree of this substitution. These results were interpreted in terms of rehybridizations of the nitrogen lone-pair orbital, changes in the highest occupied molecular orbital–lowest unoccupied (HOMO–LUMO) gap, and back-donation to the $p\pi$ orbital on boron. In this context, we have studied the attractor effect and the donor effect substitution of hydrogen's boron or hydrogen's ligand. Similar results were obtained as reported previously.¹⁸

In spite of the simplicity of the donor–acceptor bond model, the mode of coordination between Lewis acids and bases was not completely elucidated and is still controversial. Of particular

* Corresponding author.

[⊗] Abstract published in *Advance ACS Abstracts*, September 1, 1997.

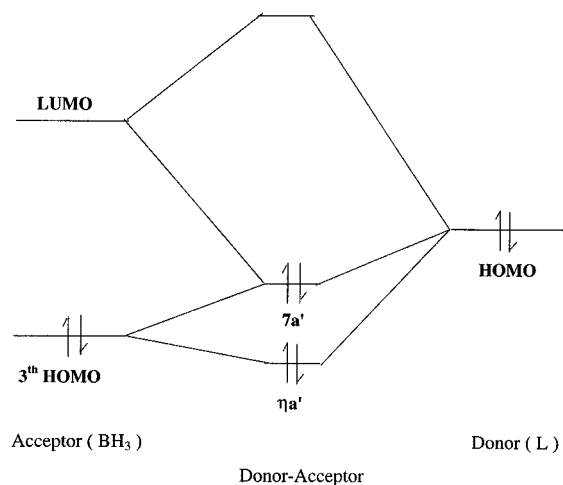


Figure 1. The scheme of donor-acceptor interaction for the three-level model (3OM-4e⁻).

interest is whether or not the donor-acceptor interaction is reduced to the simple interaction that occurs in the two-level model system. In the case of H₃BXH_{*n*} (*n* = 3, 2, and 1) complexes, it was shown that the interaction occurs between the vacant orbital of BH₃ (LUMO) and the lone-pair orbital of XH_{*n*} (HOMO). This description is not completely correct, since the interaction occurs between two molecular orbitals of the acceptor (LUMO and the occupied deeper orbital) and the highest occupied orbital (HOMO) of the donor XH_{*n*} (i.e., a three-level and four-electron model system¹⁹ (see Figure 1)). In this way, we present in this paper a qualitative molecular orbital description of the nature of the interaction between the boron hydride acceptor and Lewis base donor XH_{*n*} (X = N, O, and F). Fortunately, with recent advances in theoretical methods, the structure and the energies of small gas phase species can be calculated to within 1–2 kcal/mol.

We have made calculations at the G-2 level of theory to estimate the complexation energies of the H₃BXH_{*n*} or [H₃BXH_{*n-1*}]⁻ adducts (X = (N,P), (O,S), and (F,Cl)). The relative stabilities of these complexes are examined with respect to the qualitative molecular orbital analysis (QMOA). The QMOA arguments have proved useful and successful for predicting the broad outlines of calculations.^{20,21} They enhance understanding of the relationship between the approximate orbitals we visualize and the detailed results produced by the ab initio calculations. The choice of the complexes investigated was made with the aim to include all different types of strongly bound molecules and van der Waals complexes. A linear correlation between the complexation energies of the complexes and the G-2 calculated proton affinity of XH_{*n*} and [XH_{*n-1*}]⁻ is established and discussed. Finally, another linear correlation is established between the experimental ¹¹B NMR coupling constant ¹J_{B-H} and the complexation energies determined at the G-2 level of theory.

2. Computational Methods

Molecular orbital calculations were carried out using the GAUSSIAN 92²² series of programs with a variety of basis sets of split valence quality and with multiple polarization and diffuse functions.²³ Equilibrium geometries were optimized at the HF/6-31G(d) level of theory. Vibrational frequencies and zero-point energies (ZPEs) were calculated at the HF/6-31G(d) level using the Hartree-Fock (HF) optimized geometries and analytical second derivatives²⁴ (the ZPE value is scaled by the empirical factor 0.893).²⁵ The HF geometries obtained in the previous step were then refined at the MP2/6-31G(d) level. The G-2

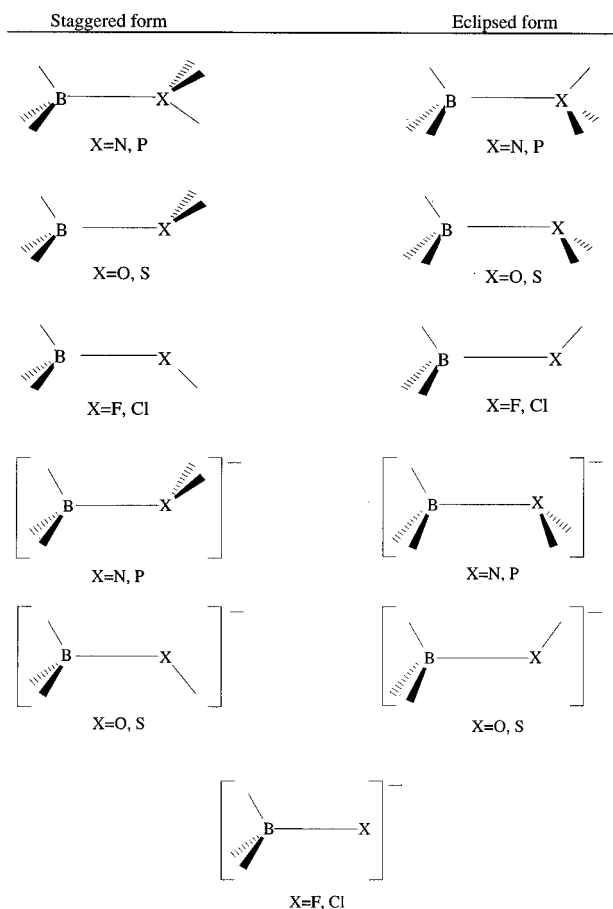


Figure 2. The staggered and eclipsed conformations of the H₃BL complexes.

theory^{26,27} is a composite one, based on the 6-311G(d,p) basis set and several basis extensions. Treatment of electron correlation is by Möller-Plesset (MP) perturbation theory and quadratic configuration interaction (QCI). The final energies are effectively at the QCISD(T)/6-311+G(3df,2p) level, making certain assumptions about additivity and appending a small higher-level empirical correction (HLC) to accommodate remaining deficiencies. This theoretical scheme has been proved²⁸⁻³⁰ to yield ionization energies, atomization energies, proton affinities, and heats of formation in agreement with the experimental values to within 0.1 eV. In this respect, it should be noted that in calculating proton affinities and complexation energies, the HLC term cancels out, and therefore, the resulting proton affinities and complexation energies are purely ab initio.

3. Results and Discussion

3.1. Geometries. Figure 2 schematically presents the possible structures (staggered and eclipsed conformations) for the complexes H₃BXH_{*n*} and [H₃BXH_{*n-1*}]⁻. Table 1 lists selected bond lengths (*d*_{B-X}, *d*_{B-H}, and *d*_{X-H}) for the complexes optimized at the MP2(full)/6-31G(d) level. The G-2 total energies and the energy differences between the two conformations of all complexes are presented in Table 2. The total optimized geometrical parameters of all complexes considered in this study are available from the authors upon request. Although a detailed discussion of the geometries of these species is not the aim of this paper, several features should be singled out for comment.

For all compounds, except for H₃BFH, the staggered conformation corresponds to a minimum and the eclipsed form corresponds to a transition state, the imaginary frequency being the torsional mode around the B-X bond. The energy

TABLE 1: MP2(full)/6-31G(d) Bond Length (Å) of Complexes

complex	symmetry	d_{B-X}		d_{B-H}^a	d_{X-H}^b
		staggered	eclipsed		
H ₃ BNH ₃	C _{3v}	1.660	1.687	1.209	1.020 (1.017)
H ₃ BOH ₂	C _s	1.730	1.752	1.207	0.975 (0.969)
H ₃ BFH	C _s	2.009	2.022	1.199	0.942 (0.934)
H ₃ BPH ₃	C _{3v}	1.943	1.974	1.206	1.404 (1.415)
H ₃ BSH ₂	C _s	2.026	2.078	1.201	1.341 (1.339)
H ₃ BClH	C _s	2.702	2.748	1.193	1.281 (1.280)
[H ₃ BNH ₂] ⁻	C _s	1.579	1.592	1.253	1.024 (1.043)
[H ₃ BOH] ⁻	C _s	1.517	1.523	1.236	0.969 (0.980)
[H ₃ BF] ⁻	C _{3v}		1.462	1.244	
[H ₃ BPH ₂] ⁻	C _s	1.999	2.023	1.222	1.429 (1.436)
[H ₃ BSH] ⁻	C _s	1.973	1.989	1.221	1.346 (1.353)
[H ₃ BCl] ⁻	C _{3v}		1.954	1.209	

^a $d_{B-H} = 1.191$ Å for isolated BH₃, computed at the MP2(full)/6-31G(d) level. ^b Values in parentheses correspond to the free ligand bond length (Å).

TABLE 2: Total Energies (E_{Tot} in au) of Complexes and ΔE (in kcal/mol)^a Computed at the G-2 Level of Theory

complex	E_{Tot}		ΔE^a
	staggered	eclipsed	
H ₃ BNH ₃	-83.025 03	-83.020 82	2.64
H ₃ BOH ₂	-102.873 28	-102.872 77	0.32
H ₃ BFH	-126.876 68	-126.876 77	-0.06
H ₃ BPH ₃	-369.236 61	-369.233 18	2.15
H ₃ BSH ₂	-425.474 72	-425.472 28	1.53
H ₃ BClH	-486.869 20	-486.8686 94	0.16
[H ₃ BNH ₂] ⁻	-82.458 52	-82.456 56	1.23
[H ₃ BOH] ⁻	-102.346 98	-102.346 45	0.33
[H ₃ BF] ⁻		-126.387 78	
[H ₃ BPH ₂] ⁻	-368.700 38	-368.697 59	1.75
[H ₃ BSH] ⁻	-424.962 56	-424.961 75	0.51
[H ₃ BCl] ⁻		-486.388 40	

^a Energy difference between the eclipsed and the staggered conformation.

difference between the two conformations is very small and gives the ligand rotational barrier (see Table 2). However, the ligand rotational barrier decreases as the electronegativity of X increases. In all complexes, the B–X bond length is moderately longer for the eclipsed conformation (see Table 1). For the anionic adducts the B–X bond length is close to a covalent bond length. The values for H₃BNH₂⁻, H₃BOH⁻, and H₃BF⁻ are 1.579, 1.517, and 1.462 Å, respectively, close to the sum of the two covalent radii of the B and X atoms (1.54, 1.53, and 1.52 Å for B–N, B–O, and B–F, respectively). However, the values for H₃BPH₂⁻, H₃BSH⁻, and H₃BCl⁻ are 1.999, 1.973, and 1.954 Å, respectively, larger than the sum of the two covalent radius of “B” and “X” atoms (1.86, 1.82, and 1.79 Å for B–P, B–S, and B–Cl, respectively). The B–H bond is longer in complexes than in isolated BH₃. This is reasonable because in BH₃ boron is hybridized sp², while the hybridization changes toward sp³ in the donor–acceptor complexes. Upon coordination, the MP2 bond length of X–H becomes shorter by 0.019 and 0.011 Å for NH₂⁻ and OH⁻, respectively, and 0.006 and 0.007 Å for PH₂⁻ and SH⁻, respectively.

For the neutral adducts, the B–X bond lengths are longer than the corresponding anionic B–X bond lengths. These distances increase as the electronegativity of X increases and vary from pseudo-covalent bonds to van der Waals bonds: the optimized values at the MP2(full)/6-31G(d) are 1.660, 1.730, and 2.009 Å for B–N, B–O, and B–F, respectively, compared to the corresponding van der Waals bond $d_{B-Ne} = 2.627$ Å (value obtained at the MP2(full)/6-31G(d) level).³¹ For B–P, B–S, and B–Cl, the optimized values are 1.943, 2.026, and

TABLE 3: Comparison of Present G-2 Dissociation Energy (in kcal/mol) with Experimental and Other Accurate Theoretical Calculations for the H₃BNH₃ Complex

	D_e	D_0^a	ref
G-2	31.4	26.08	this work
MP4/6-311G*/MP3/6-31G*	34.7		44
MP2/TZ2P	33.7	28.30	15
MP2/TZ2P		30.7 ^b	15
DFT	32.8	26.30	45
NL-SCF ^c	32.1	26.80	46
CCSD(T)(aug-cc-pVTZ) ^d	31.1	24.6	45
expt ^e	31.1		47

^a D_0 values include the ZPE correction. ^b Includes thermal corrections. ^c Local density approximation with nonlocal corrections to the correlation and exchange potentials. ^d CCSD(T)/(augmented-correlation-consistent-polarized-valence triplet-zeta) calculations. ^e Estimated value.

TABLE 4: Proton Affinities (PA in kcal/mol)^a of Ligands (L = XH_n and [XH_{n-1}]⁻) and Complexation Energies (E_c in kcal/mol)^b of Complexes Computed at the G-2 level of theory and Experimental Proton Affinities (PA_(exp) in kcal/mol)

complex	E_c^b	PA ^a	PA _(exp)
H ₃ BNH ₃	-26.08	204.2	203.4 ^c
H ₃ BOH ₂	-10.30	164.7	164.9 ^c
H ₃ BFH	-1.22	116.0	117.0 ^d
H ₃ BPH ₃	-20.56	188.4	188.6 ^d
H ₃ BSH ₂	-12.02	169.3	168.7 ^c
H ₃ BClH	-2.64	134.9	133.0 ^c
[H ₃ BNH ₂] ⁻	-72.96	402.4	
[H ₃ BOH] ⁻	-68.65	388.6	
[H ₃ BF] ⁻	-64.18	369.8	
[H ₃ BPH ₂] ⁻	-50.59	366.5	
[H ₃ BSH] ⁻	-41.52	350.9	
[H ₃ BCl] ⁻	-34.26	333.3	

^a PA(L) = $-[E(LH^+) - E(L)]$. ^b $E_c = E(H_3BL) - [E(H_3B) + E(L)]$ with L = XH_n and [XH_{n-1}]⁻. (The E_c values include ZPE corrections.) ^c Reference 48. ^d Reference 49.

2.702 Å, respectively, compared to the corresponding van der Waals bond $d_{B-At} = 3.232$ Å (value obtained at the MP2(full)/6-31G(d) level).³¹ Upon complexation, the MP2 B–H and X–H bond values are slightly longer than isolated fragments.

3.2. Complexation Energy. Table 3 presents the G-2 computed binding energy of the classical donor–acceptor complex H₃BNH₃ along with experimental values and previous high-level theoretical calculations. Our G-2 result is in good agreement with the experimental values and with all previous calculations. In Table 4, we give the complexation energies corresponding to the reaction of boron hydride BH₃ and the ligands XH_n or [XH_{n-1}]⁻ ($n = 1-3$) to form the electron donor–acceptor complexes H₃BXH_n or [H₃BXH_{n-1}]⁻ (it is taken as the energy difference between the complex and the dissociation products). The formation of the intermolecular bond involves the donation of charge density from the donor XH_n or [XH_{n-1}]⁻ to boron hydride, BH₃. Table 4 also gives the corresponding ligand proton affinities (i.e., the energy difference between the neutral and protonated ligand) which can be taken as a quantitative measure of the charge transferred from the ligand to boron hydride. It was mentioned in the Introduction that this proton affinity was proportional to the complexation energy.

G-2 results show that the H₃BXH₃ (X = N, P) complexes are more stable than the H₃BXH₂ (X = O, S) and the H₃BXH (X = F, Cl) ones (see Table 4). For the anionic adducts, the order of stability is different: [H₃BXH_{n-1}]⁻ (X = N, O, F) are more stable than [H₃BXH_{n-1}]⁻ (X = P, S, Cl and $n = 3, 2, 1$) (see Table 4). Therefore, the anionic donor–acceptor complexes show rather strong donor–acceptor bonds compared to

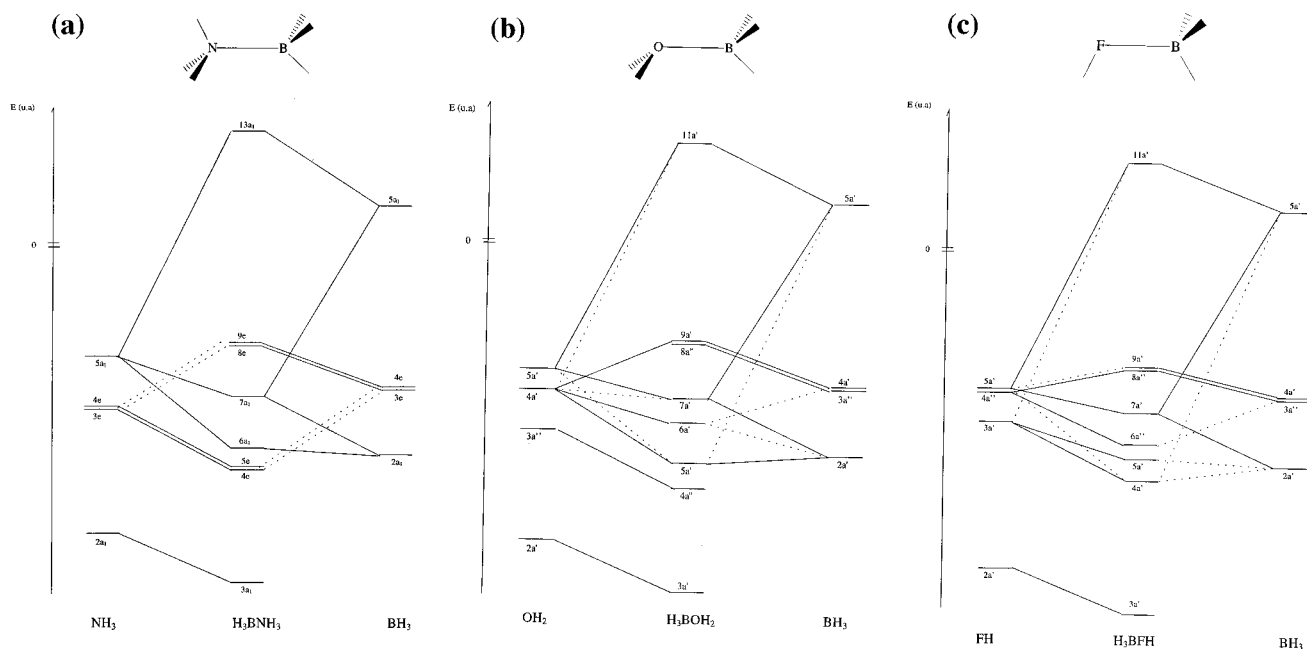


Figure 3. Fragmental analysis of the molecular orbitals of (a) H_3BNH_3 , (b) H_3BOH_2 , and (c) H_3BFH .

the corresponding neutral adducts. These values can be explained since H_3BXH_2^- , H_3BXH^- , and H_3BX^- are isoelectronic to the corresponding stable organic compounds CH_3XH_2 , CH_3XH , and CH_3X ($\text{X} = (\text{N}, \text{P}), (\text{O}, \text{S}),$ and (F, Cl)), respectively, and in the anionic ligands, the HOMO is high in energy. Furthermore, in the anionic complexes, the central atom X of the donor is in its preferred coordination.

3.3. The Qualitative Molecular Orbital Analysis. The energetic information given in table 4 brings out several questions: What is the origin of the stabilization upon complexation? Why are the H_3BXH_3 ($\text{X} = \text{N}, \text{P}$) complexes more stable than the H_3BXH_2 ($\text{X} = \text{O}, \text{S}$) and H_3BXH ($\text{X} = \text{F}, \text{Cl}$) ones, in spite of the fact that all ligands have the same number of valence electrons and the same hybridization for the base centers, X (sp^3)? The answers to these questions are directly related to the molecular orbital redistribution which takes place upon coordination. In this section, we apply QMOA to illustrate the two moieties that influence their stabilities. For the sake of simplicity, we shall start our analysis with the H_3BNH_3 , H_3BOH_2 , and H_3BFH complexes.

We shall now discuss the characteristics of the chemical bond in the molecules under consideration from an ab initio calculation at the HF/STO-3G level of theory (this basis set has been chosen only for qualitative interpretations).

Parts a–c of Figure 3 illustrate the fragmental analysis of molecular orbitals (the connecting lines indicate interactions stronger than 15%, and when it is weaker than 15%, the corresponding line is dashed) that generally influences the molecular bonding of H_3BNH_3 , H_3BOH_2 , and H_3BFH , respectively. In all correlation diagrams, the molecular orbitals of BH_3 and the ligands (NH_3 , OH_2 , FH) were taken in the symmetry of the corresponding complex.

For the H_3BNH_3 complex, the qualitative molecular orbital model (Figure 3a) allows the assertion that $6a_1$ and $7a_1$ are those MOs that are responsible for the chemical bond between the fragments NH_3 and BH_3 . The $6a_1$ orbital is mainly formed by the $2a_1$ MO (i.e., the acceptor-occupied orbital) and the $5a_1$ (HOMO) MO of NH_3 . On the other hand, the $7a_1$ orbital of the complex results from interaction between the acceptor-occupied $2a_1$ orbital and the LUMO $5a_1$ orbital of the BH_3 fragment and the $5a_1$ HOMO of NH_3 . The nitrogen contribution

to the $7a_1$ orbital is larger than the boron contribution, and this orbital has a bonding character with respect to nitrogen and boron atoms. Therefore, this latter complex MO can be compared with the bonding orbital in the two-level donor–acceptor interaction, being the $13a_1$ orbital of the complex antibonding orbital whose contribution to the boron hydride is larger than the contribution to the ammonia. According to the fragment calculations, this MO is predominantly formed by the $5a_1$ LUMO of BH_3 and the $5a_1$ HOMO of NH_3 . Hence, we can consider the $13a_1$ MO as the closest one in character to the antibonding orbital of the two-level donor–acceptor bond. The other occupied MOs are similar in structure to the orbitals of the initial molecules NH_3 and BH_3 . The $3e$ and $4e$ orbitals of both BH_3 and NH_3 interact only slightly between them. We can therefore conclude that a π -bond is not formed between BH_3 and NH_3 . Similar results were obtained by Dapprich and Frenking¹⁶ using the charge decomposition analysis to explain the bond nature in the H_3BNH_3 complex. They showed that the core orbitals remain nearly unchanged upon complexation between BH_3 and NH_3 moieties. The large contributions to donor–acceptor interactions are calculated for the $6a_1$ and $7a_1$ MOs. Furthermore, their results proved that the charge donation from NH_3 to BH_3 is mainly due to the $7a_1$ MO (0.283 and, 0.367 e at HF/6-31G(d) and MP2/6-31G(d), respectively), and there is no back-donation from BH_3 to NH_3 . They also showed that there is a large depletion of electronic charge in the overlapping region of the occupied orbitals of BH_3 and NH_3 , that form $7a_1$ MO (−0.643 and −0.269 e at HF/6-31G(d) and MP2/6-31G(d), respectively). In addition, the $6a_1$ orbital shows an accumulation of electronic charge (0.342 and −0.267 e at HF/6-31G(d) and MP2/6-31G(d), respectively) in the occupied/occupied overlap region of the fragments.

In the case of the H_3BOH_2 complex, the correlation diagram (Figure 3b) shows that the B–O bond is formed with the participation of the first and second HOMO, $5a'$ and $4a'$, respectively, of the H_2O and the occupied orbitals $2a'$, $4a'$, and the LUMO $5a'$ of BH_3 . These MOs lead to formation of five orbitals $5a'$, $6a'$, $7a'$, $9a'$, and $11a'$, and they reflect the complex B–O bond. Other occupied MOs are similar in structure to the orbitals of the initial molecules H_2O and BH_3 . The interaction between the $4a'$ orbital of H_2O and the $4a'$ orbital

of BH_3 allows the B-O bond to acquire a π -character. This is reflected by the $6a'$ and $9a'$ orbitals of the complex. It should be pointed out that only one of these orbitals, $7a'$, is formed with the participation of three molecular orbitals: the unoccupied $5a'$ orbital (LUMO of BH_3) and the acceptor-occupied $2a'$ and $5a'$ (HOMO of H_2O) orbitals. In contrast to other MOs, the contribution of the oxygen atomic orbitals (AOs) to the $7a'$ MO is larger than the contribution of the boron AOs. Therefore, with some approximation, this MO can be correlated with the bonding orbital of the two-level model of the donor-acceptor bond, while the $11a'$ MO can be treated as the antibonding orbital for this same model.

The fragmental analysis of the H_3BFH complex (Figure 3c) shows that σ - and π -bonds are characteristic. The latter are described by the $6a''$, $8a''$, and $9a'$ MOs, in which the $4a''$ and $5a'$ orbitals of FH participate, while the σ -bonds are described by the $4a'$ and $7a'$ MOs of the complex. The formation of the $7a'$ orbital, which represents the B-F bond, results from the interaction of the occupied acceptor $2a'$ orbital and the LUMO $5a'$ orbital of BH_3 with the HOMO $5a'$ orbital of FH. In this MO, the contribution of fluorine is larger than the contribution of boron, therefore the $7a'$ MO can be compared to the bonding orbital of two-level model of the donor-acceptor interaction.

Comparing these three correlation diagrams of the H_3BNH_3 , H_3BOH_2 , and H_3BFH complexes, we can reach the conclusion that the qualitative molecular orbital model indicates that an occupied orbital of the boron fragment also contributes to the "X-Boron" σ -bond. Hence, the X-Boron chemical bond cannot be reduced to the two-level model system. In actual compounds, the interaction occurs between the occupied orbital of the donor and the acceptor. The contribution of the occupied acceptor orbital in the interaction with the donor reduces the stability of the complex. Thus, this comparison shows that the LUMO-HOMO gap is an important factor in influencing the stability of electron donor-acceptor complexes. In fact, when the LUMO-HOMO gap increases, the complex stability decreases (the LUMO-HOMO gaps are 2.77, 3.69, and 5.07 kcal/mol for H_3BNH_3 , H_3BOH_2 , and H_3BFH , respectively). The type of interaction for these adducts is described as a three-level and four-electron system: "3OM-4e⁻" (see Figure 1).

3.4. Correlations. In parts a and b of Figure 4, we present the linear correlation between the proton affinities of the ligand, XH_n or $[\text{XH}_{n-1}]^-$, and the complexation energies of H_3BL ($\text{L} = \text{XH}_n$ or $[\text{XH}_{n-1}]^-$) using G-2 calculations.

Recently, Frenking and co-workers¹⁵ have shown that there is no correlation between the charge transfer and the bond strength in donor-acceptor complexes from the NBO analysis. We think that this result comes from the large variety of acceptor and nature of the ligand used. The proton affinity (as to what was mentioned above) can be taken as a quantitative measure of the charge transferred to the boron hydride from the ligand. Figure 4a,b shows a good linear correlation between proton affinities and complexation energies. This correlation reflects that the stability of the complex depends completely on the nature of ligands. This stability increases when the basicity of the Lewis bases increases.

In 1957, Rice³² discussed a correlation between $\nu_{\text{B-H}}$ and stability for a series of H_3BL compounds. Other authors³³⁻³⁵ have commented on the relationship between $^1J_{\text{B-H}}$ and the boron "s" character in the boron hydrogen bond. Watanabe³⁶ has discussed the linear relationship between the weighted average of $\nu_{\text{B-H}}$ and $^1J_{\text{B-H}}$ for an extensive series of boron compounds. A study by Berschied and Purcell³⁷ showed that it is possible to use this correlation to infer qualitative features

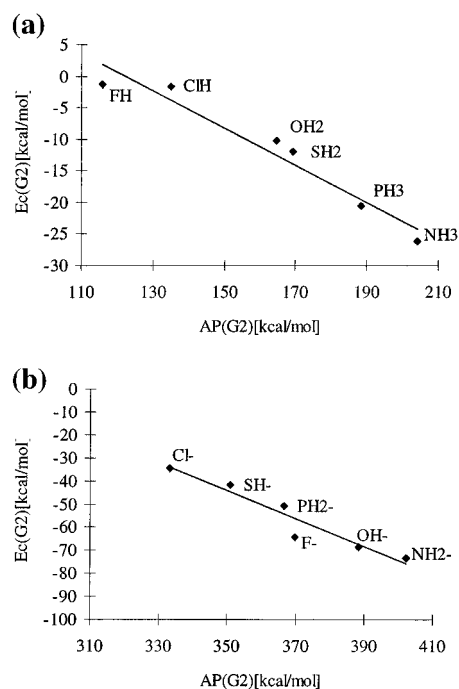


Figure 4. Linear correlation between G-2 proton affinities and the complexation energies of (a) H_3BXH_n and (b) $[\text{H}_3\text{BXH}_{n-1}]^-$ complexes.

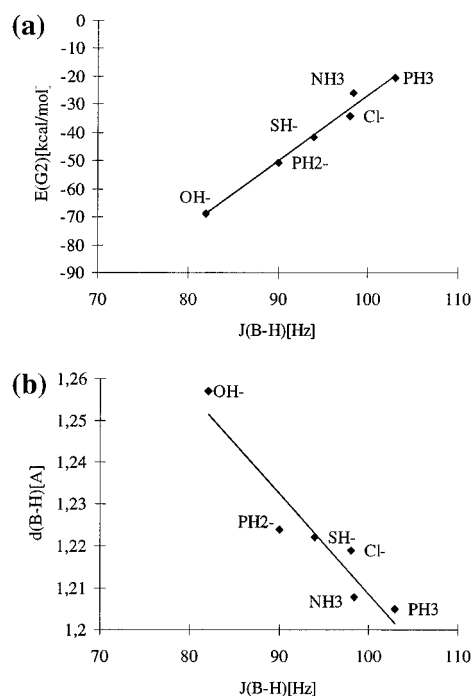


Figure 5. Linear correlation between the experimental coupling constant $^1J_{\text{B-H}}$ and (a) the G-2 complexation energies and (b) the MP2 $d_{\text{B-H}}$ bond lengths of the complexes.

of the "B-L" bonding and to assess the stability of the corresponding adducts.

In this work, we report two linear correlations, the first one is between the ^{11}B NMR coupling constant $^1J_{\text{B-H}}$ (experimental factor reflecting the rigidity of the B-H bond) and the complexation energies of the H_3BL complexes ($\text{L} = \text{OH}^-$, PH_2^- , SH^- , Cl^- , NH_3 , PH_3) calculated at the G-2 level of theory (see Figure 5a). This correlation shows that the interaction between BH_3 and ligands is important, i.e., the complexes show great stability, when the coupling constant $^1J_{\text{B-H}}$ is low. Thus, the bond length B-H becomes longer than that in isolated BH_3 (1.191 Å value obtained at the MP2/6-31G(d) level). This latter

observation allows the establishment of a second linear correlation between the same coupling constant $^1J_{B-H}$ and the B-H bond length determined at the MP2(full)/6-31G(d) level (see Figure 4b).

All the correlations are verified for the H_3BL complexes for which spectroscopic data are available ($L = OH^-, PH_2^-, SH^-, Cl^-, NH_3, PH_3$).³⁸⁻⁴³

4. Conclusion

The study of H_3BL complexes, obtained from the association of the acceptor boron hydride and the donor ligands XH_n or $[XH_{n-1}]^-$ ($X = N, O, F, P, S,$ and Cl) at the G-2 level of theory, leads to following results: H_3BL complexes prefer the staggered form, except the H_3BFH complex which prefers the eclipsed conformation. The analysis of correlation diagrams of the H_3BXH_n ($X = N, O, F$) complexes shows that the σ -character of the B-X bond decreases and the π -character increases when the electronegativity of X increases. Thus, the contribution of the occupied acceptor orbital in the interaction with the donor results in a decrease in the stability of the complex. This stability depends completely on the nature of the ligands. In fact, linear correlation between proton affinity of the ligand and complexation energy is derived. In the neutral complexes, the bonding can be classified as intermediate between a pseudo-covalent and a van der Waals type of bond, but in the anionic complexes the bonding is of covalent type. The neutral complexes H_3BXH_n are less stable than the corresponding anionic ones $[H_3BXH_{n-1}]^-$. Finally, two linear correlations were established: the first one was between the ^{11}B NMR coupling constant $^1J_{B-H}$ and the complexation energies of the H_3BL complexes ($L = OH^-, PH_2^-, SH^-, Cl^-, NH_3, PH_3$), and the second one was between the same coupling constant and the B-H bond length obtained at the MP2(full)/6-31G(d) level of calculation.

Acknowledgment. We thank Prof. I. Nebot-Gil for helpful discussions and for critical reading of the manuscript. We greatly appreciate the financial support provided by the DGICYT from Spain, Project PB94-0993.

References and Notes

- Pellon, P. *Tetrahedron Lett.* **1992**, 31, 4451.
- Lang, A.; Noth, H.; Schmidt, M. *Chem. Ber.* **1995**, 128, 751.
- Stock, A.; Massenez, C. *Chem. Ber.* **1912**, 45, 3539.
- Muetterties, E. *Boron Hydride Chemistry*; Academic Press: New York, 1975.
- Lane, C. F. *Chem. Rev.* **1976**, 76, 773.
- Carpenter, J. D.; Ault, B. S. *J. Phys. Chem.* **1991**, 95, 3502 and references cited therein.
- Carpenter, J. D.; Ault, B. S. *J. Mol. Struct.* **1993**, 298, 17.
- Carpenter, J. D.; Ault, B. S. *J. Phys. Chem.* **1992**, 96, 7913.
- Carpenter, J. D.; Ault, B. S. *J. Phys. Chem.* **1991**, 95, 3507.
- Carpenter, J. D.; Ault, B. S. *J. Phys. Chem.* **1992**, 96, 4288.
- Carpenter, J. D.; Ault, B. S. *J. Phys. Chem.* **1993**, 97, 3697.
- Sakai, S. *J. Phys. Chem.* **1995**, 99, 9080.
- Umeyama, H.; Morokuma, K. *J. Am. Chem. Soc.* **1976**, 98, 7208.
- Glendening, E. D.; Streitwieser, A. *J. Chem. Phys.* **1994**, 100, 2900.
- Jonas, V.; Frenking, G.; Reetz, M. T. *J. Am. Chem. Soc.* **1994**, 116, 8741.
- Dapprich, S.; Frenking, G. *J. Phys. Chem.* **1995**, 99, 9352.
- Skandke, A.; Skandke, P. N. *J. Phys. Chem.* **1996**, 100, 15079.
- Anane, H.; Boutalib, A.; Tomás, F. Manuscript in preparation.
- Anane, H.; Boutalib, A. Presented to QTEL'96, Spain, September 16-20, 1996.
- Lowe, J. P. *Quantum Chemistry*; Academic Press: New York, 1978.
- Gimarc, B. M. *Molecular Structure and Bonding*; Academic Press: New York, 1979.
- Frisch, M. J.; Trucks, G. W.; Head-Gordon, M.; Gill, P. M. W.; Wong, M. W.; Foresman, J. B.; Johnson, B. G.; Schlegel, H. B.; Robb, M. A.; Replogle, E. S.; Gomperts, R.; Andres, J. L.; Raghavachari, K.; Binkley, J. S.; Gonzalez, C.; Martin, R. L.; Fox, D. J.; Defrees, D. J.; Baker, J.; Stewart, J. J. P.; Pople, J. A. *GAUSSIAN 92*; Gaussian, Inc.: Pittsburgh, PA, 1992.
- Hariharan, P. C.; Pople, J. A. *Theor. Chim. Acta.* **1973**, 28, 213 and references cited therein. Francl, M. M.; Pietro, W. J.; Hehre, W. J.; Binkley, J. S.; Gordon, M. S.; Defrees, D. J.; Pople, J. A. *J. Chem. Phys.* **1982**, 77, 3654. Frisch, M. J.; Pople, J. A.; Binkley, J. S. *J. Chem. Phys.* **1984**, 80, 3265 and references cited therein.
- Pople, J. A.; Krishnan, R.; Schlegel, H. B.; Binkley, J. S. *Int. J. Quantum Chem. Symp.* **1979**, 13, 225.
- Pople, J. A.; Schlegel, H. B.; Krishnan, R.; Defrees, D. J.; Binkley, J. S.; Frisch, M. J.; Whiteside, R. A.; Hout, R. F.; Hehre, W. J. *Int. J. Quantum Chem., Quantum Chem. Symp.* **1981**, 15, 269.
- Curtiss, L. A.; Raghavachari, K.; Trucks, G. W.; Pople, J. A. *J. Chem. Phys.* **1991**, 94, 7221.
- For reviews, see: Curtiss, L. A.; Raghavachari, K. In *Quantum Mechanical Electronic Structure Calculations with Chemical Accuracy*; Langhoff, S. R., Ed.; Kluwer Academic: Dordrecht, The Netherlands, 1995; p 139; Raghavachari, K.; Curtiss, L. A. In *Modern Electronic Structure Theory*; Yarkony, D. R., Ed.; World Scientific: Singapore, 1995, p 991.
- Curtiss, L. A.; Carpenter, J. E.; Raghavachari, K.; Pople, J. A. *J. Chem. Phys.* **1992**, 96, 9030.
- Smith, B. J.; Radom, L. *J. Am. Chem. Soc.* **1993**, 115, 4885.
- Curtiss, L. A.; Raghavachari, K.; Pople, J. A. *J. Chem. Phys.* **1993**, 98, 1293.
- Boutalib, A. Unpublished results.
- Rice, B.; Galiano, R. J.; Lehmann, W. J. *J. Phys. Chem.* **1957**, 61, 1222.
- Phillips, W. D.; Miller, H. C.; Muetterties, E. L. *J. Am. Chem. Soc.* **1959**, 81, 4496.
- Gutowsky, H. S.; McCall, O. W.; Slichter, C. P. *J. Am. Chem. Soc.* **1953**, 75, 4567.
- Onak, T. P.; Landesman, H.; Williams, R. E.; Shapiro, I. *J. Phys. Chem.* **1959**, 63, 1533.
- Watanabe, H.; Nagasawa, K. *J. Phys. Chem.* **1967**, 6, 1068.
- Berschied, J. R.; Purcell, K. F. *Inorg. Chem.* **1970**, 9, 624.
- Gardiner, J. A.; Collat, J. W. *J. Am. Chem. Soc.* **1964**, 86, 3165.
- Noth, H.; Wrackmeyer, B. *Chem. Ber.* **1974**, 107, 3070.
- Rudolph, R. W.; Parry, R. W.; Farran, C. F. *Inorg. Chem.* **1966**, 5, 723.
- Spielvogel, B. F.; Rothgery, E. F. *J. Chem. Soc., Chem. Commun.* **1966**, 765.
- Dietz, E. A.; Morse, K. W.; Parry, R. W. *Inorg. Chem.* **1976**, 15, 1.
- Lawrence, S. H.; Shore, S. G.; Koetzle, T. F.; Huffman, J. C.; Wei, C. Y.; Bau, R. *Inorg. Chem.* **1985**, 24, 3171.
- Binkley, J. S.; Thorne, L. R. *J. Chem. Phys.* **1983**, 79, 2932.
- Bauschlicher, C. W., Jr.; Ricca, A. *Chem. Phys. Lett.* **1995**, 237, 14.
- Branchadell, V.; Sbai, A.; Oliva, O. *J. Phys. Chem.* **1995**, 99, 6472.
- Haaland, A. *Angew. Chem., Int. Ed. Engl.* **1989**, 28, 992.
- Szulejko, J. E.; McMahon, T. B. *J. Am. Chem. Soc.* **1993**, 115, 7839.
- Lias, S. G.; Bartmess, J. E.; Liebman, J. F.; Holmes, J. L.; Levin, R. D.; Mallard, W. G. *J. Phys. Chem. Ref. Data Suppl.* **1988**, 1, 17.